On cerebral lupus: from pathogenesis to clinical outcomes

Magro Checa, C.

7

GLIAL AND AXONAL CHANGES IN SYSTEMIC LUPUS ERYTHEMATOSUS MEASURED WITH DIFFUSION OF INTRACELLULAR METABOLITES

Ercan E, Magro-Checa C, Valabregue R, Branzoli F, Wood ET, Steup-Beekman GM, Webb AG, Huizinga TW, van Buchem MA, Ronen I.

Brain. 2016 May;139(Pt 5):1447-57.

ABSTRACT

Systemic lupus erythematosus is an inflammatory autoimmune disease with multi-organ involvement. Central nervous system involvement in systemic lupus erythematosus is common and results in several neurological and psychiatric symptoms that are poorly linked to standard magnetic resonance imaging outcome. Magnetic resonance imaging methods sensitive to tissue microstructural changes, such as diffusion tensor imaging and magnetization transfer imaging, show some correlation with neuropsychiatric systemic lupus erythematosus (NP-SLE) symptoms. Histological examination of NP-SLE brains reveals presence of cerebral oedema, loss of neurons and myelinated axons, microglial proliferation and reactive astrocytosis, microinfacrts and diffuse ischaemic changes, all of which can affect both diffusion tensor imaging and magnetization transfer imaging in a non-specific manner. Here we investigated the underlying cell-type specific microstructural alterations in the brain of patients with systemic lupus erythematosus with and without a history of central nervous system involvement. We did so combining diffusion tensor imaging with diffusion-weighted magnetic resonance spectroscopy, a powerful tool capable of characterizing cell-specific cytomorphological changes based on diffusion of intracellular metabolites. We used a 7 T magnetic resonance imaging scanner to acquire T1-weighted images, diffusion tensor imaging datasets, and single volume diffusion-weighted magnetic resonance spectroscopy data from the anterior body of the corpus callosum of 13 patients with systemic lupus erythematosus with past NP-SLE, 16 patients with systemic lupus erythematosus without past NP-SLE, and 19 healthy control subjects. Group comparisons were made between patients with systemic lupus erythematosus with/without past NP-SLE and healthy controls on diffusion tensor imaging metrics and on diffusion coefficients of three brain metabolites: the exclusively neuronal/axonal N-acetylaspartate, and the predominantly glial creatine + phosphocreatine and choline compounds. In patients with systemic lupus erythematosus with past NP-SLE, significantly higher diffusion tensor imaging mean and radial diffusivities were accompanied by a significantly higher intracellular diffusion of total creatine (0.202 ± 0.032 μm^2/ms, P=0.018) and total choline (0.142 ± 0.031 μm^2/ms, P=0.044) compared to healthy controls (0.171 ± 0.024 μm^2/ms, 0.124 ± 0.018 μm^2/ms, respectively). Total N-acetylaspartate, total creatine and total choline diffusion values from all patients with systemic lupus erythematosus correlated positively with systemic lupus erythematosus disease activity index score (P=0.033, P=0.040, P=0.008, respectively). Our results indicate that intracellular alterations, and in particular changes in glia, as evidenced by increase in the average diffusivities of total choline and total creatine, correlate with systemic lupus erythematosus activity. The higher diffusivity of total creatine and total choline in patients with NP-SLE, as well as the positive correlation of these diffusivities with the systemic lupus erythematosus disease activity index are in line with cytomorphological changes in reactive glia, suggesting that the diffusivities of choline compounds and of total creatine are potentially unique markers for glial reactivity in response to inflammation.

Systemic lupus erythematosus (SLE) is a female predominant autoimmune disease that affects multiple organs.(1) Central nervous system (CNS) involvement in SLE is common and results in several neurological and psychiatric symptoms. These symptoms are poorly characterized by standard magnetic resonance imaging (MRI), which appears normal in about 50% of patients with neuropsychiatric systemic lupus erythematosus (NP-SLE). Focal lesions and vascular infarcts, visible on MRI of patients with NP-SLE, are non-specific and often do not correlate with clinical outcome and with symptom severity.(2)

MRI methods sensitive to tissue microstructural changes, such as diffusion tensor imaging (DTI) and magnetization transfer imaging (MTI), show diffuse white matter changes that correlate with the clinical status of patients with NP-SLE.(3-7) Histological examination of NP-SLE brains has revealed the presence of cerebral oedema, loss of neurons and myelinated axons, microglial proliferation and reactive astrocytosis, microinfarcts and diffuse ischemic changes, all of which can affect the image contrast in DTI and MTI.(8) Therefore, although clinically informative, due to the lack of specificity, these imaging modalities provide limited insight into the microstructural deficit in NP-SLE.

Magnetic resonance spectroscopy (MRS) reports on concentrations of cell-specific metabolites, and MRS studies have shown differences in the concentrations (relative to total creatine) of several brain metabolites, including significantly lower N-Acetylaspartate (NAA) and significantly higher choline and myo-inositol levels in patients with SLE and NP-SLE compared to healthy controls.(9,10) In addition, one study reported significantly lower NAA in SLE patients with high disease activity compared to those with low disease activity.(11) Although MRS provides cell-type specific information, it does not provide any structural information.

Diffusion-weighted magnetic resonance spectroscopy (DW-MRS) combines the cell-type specificity of MRS with the microstructural sensitivity of diffusion-weighted imaging (DWI), and allows studying cell- and compartment-specific properties of tissue microstructure by probing the diffusion of intracellular brain metabolites.(12,13) Of these metabolites, N-acetylaspartate typically co-measured with N-acetylaspartylglutamate (NAAG) (NAA + NAAG = tNAA) resides almost exclusively in neurons/axons; creatine and phosphocreatine (Cr + PCr = tCr), pivotal in aerobic cell energetics, are found in all neural cells, but their astrocytic concentration is twice their neuronal one, and soluble choline-containing compounds (tCho) are predominantly glial, with a glial/neuronal concentration ratio of 3:1.(14,15) The diffusion properties of these metabolites are strongly dictated by the structural and physiological features of their respective intracellular space, and thus provide a unique in-vivo probe for pathology affecting intracellular structures, such as ischemia, tumors, and axonopathy in multiple sclerosis (MS), as well as making accurate vivo cell-specific

characterization of tissue microstructure possible.(16-21)

In this study we utilize for the first time the sensitivity of DW-MRS to selectively report on axonal and glial microstructure (a) to investigate the underlying microstructural alterations in a normal appearing portion of the corpus callosum in the brain of SLE patients with and without history of NP-SLE and (b) to assess the relationship between DW-MRS indices and SLE activity in the patient population in this study. These studies were performed at ultrahigh field (7 Tesla) in order to obtain the sensitivity required for robust DW-MRS measurements.

MATERIALS AND METHODS

Human Subjects

Twenty-nine SLE patients (one male, 28 females, age: 43 ± 10 years) and 19 age- and sex-matched healthy volunteers (one male, 18 females, age: 41 ± 11 years) were included in the study. The study adhered to the Helsinki Declaration and was approved by the institutional review board of our institution. Written informed consent was obtained from all subjects prior to the study. Of 29 SLE patients, 13 had a history of NP-SLE and sixteen had no history. For convenience, patients with NP-SLE in the past are referred to as "patients with NP-SLE" throughout the text. All patients with SLE were diagnosed according to the 1982 revised American College of Rheumatology criteria.(22,23) All NP-SLE patients were diagnosed at the Leiden NP-SLE-clinic after a standardized multidisciplinary medical examination.(24) NP diagnoses were classified according to the 1999 American College of Rheumatology case definitions for NP-SLE syndromes.(25) The NP syndromes in our NP-SLE cohort included cerebrovascular disease (5 patients), seizures (3 patients), cognitive disorder (3 patients), movement disorder (1 patient), headache (2 patients), acute confusional state (3 patients), psychosis (1 patient), transverse myelitis (1 patient), polyneuropathy (1 patient), anxiety (1 patient), and radiculopathy (1 patient). In order to categorize the patients according to SLE disease activity, we calculated the systemic lupus erythematosus disease activity index 2000 (SLEDAI-2K) for each patient.(26) Permanent and irreversible damage due to SLE was assessed with the systemic lupus international collaborating clinics (SLICC)/American College of Rheumatology damage index (SDI).(27,28) SLE patients with a SLEDAI-2K $\geq$ 8 were considered to have high SLE activity and were categorized as SLE-active, while the remaining SLE patients were categorized as SLE-inactive.(11) The demographics of the study and the clinical characteristics of the SLE patients are shown in (**Table 1**).

Table 1: Patient characteristics

	NPSLE patients (n=13)	SLE patients (n=16)	*P*
Age (years)	43 ± 8	42 ± 11	0,721
SLE disease duration (years)	12 ± 9	8 ± 5	0,178
SLEDAI-2K	7 ± 6	3 ± 2	0,006
SDI	2 ± 2	1 ± 1	0,241
Patient characteristics			
Antiphospholipid syndrome	3/13 (23%)	1/16 (6%)	0,223
Presence of auto-antibodies			
Antinuclear antibody	12/13 (92%)	14/16 (88%)	0,580
Anti-ENA	9/13 (70%)	7/16 (44%)	0,160
Anti-DNA	1/13 (8%)	6/16 (38%)	0,074
Anti-RNP	3/13 (23%)	3/16 (19%)	0,565
Anti-SSA	4/13 (31%)	7/16 (44%)	0,372
Anti-SSB	1/13 (8%)	2/16 (13%)	0,580
Anti-Smith	2/13 (15%)	2/16 (13%)	0,617
Anticardiolipine Autoantibodies	3/13 (23%)	1/16 (6%)	0,223
Lupus Anticoagulant	6/13 (46%)	2/16 (13%)	0,055
Anti-B2 Glycoproteine IgG	2/13 (15%)	0/16 (0%)	0,192
Presence of ACR criteria ever in disease course			
Malar rash	5/13 (38%)	8/16 (50%)	0,404
Discoid lupus	2/13 (15%)	0/16 (0%)	0,192
Photosensitivity	5/13 (38%)	7/16 (44%)	0,537
Ulcers	7/13 (54%)	7/16 (44%)	0,434
Arthritis	12/13 (92%)	9/16 (56%)	0,038
Serositis	4/13 (31%)	6/16 (38%)	0,507
Lupus nephritis	4/13 (31%)	5/16 (31%)	0,647
Neurological disorder	4/13 (31%)	0/16 (0%)	0,448
Hematologic disorder	6/13 (46%)	8/16 (50%)	0,566
Immunologic disorder	9/13 (70%)	13/16 (81%)	0,374
Antinuclear antibodies	13/13 (100%)	16/16 (100%)	0,374
Current medication			
Prednisone	9/13 (70%)	9/16 (56%)	0,372
Azathioprine	3/13 (23%)	6/16 (38%)	0,336
Methotrexate	1/13 (8%)	1/16 (6%)	0,704
Hydroxychloroquine	11/13 (85%)	12/16 (75%)	0,435
Mycophenolate mofetil	3/13 (23%)	2/16 (13%)	0,396

ACR = American College of Rheumatology; IgG = immunoglobulin G; SDI = systemic lupus international collaborating clinics (SLICC)/American College of Rheumatology damage index.
*P<0.05; ** P<0.01.

Data Acquisition

All subjects were scanned on a 7 tesla Philips Achieva MRI scanner (Philips Healthcare, Best, The Netherlands) equipped with a 32-channel receive head coil (Nova Medical Inc., Wilmington, MA, USA). The scan protocol consisted of a short survey scan and a sensitivity encoding reference scan followed by (a) sagittal 3D T_1-weighted images (Field of view (FOV): 246×246×174 mm^3, resolution: 0.85x0.85x1 mm^3, repetition time/echo time (TR/TE): 4.00 /1.84 ms, total scan time: 1.59 min); (b) axial multislice diffusion tensor images (FOV**:** 224×224×150 mm^3, resolution: 1.75x1.75x2.20 mm^3, TR/TE: 10000/65 ms, 15 diffusion weighting directions with b = 1000 s/mm^2, total scan time: 3 min) and (c) single-volume diffusion-weighted spectroscopy scans (detailed protocol below).

DW-MRS Protocol

The DW-MRS sequence was based on the PRESS (Point Resolved Spectroscopy) sequence with bipolar diffusion-weighting gradients added on both sides of the 180° pulses. A $3cm^3$ volume of interest (VOI) (25 (AP) × 15 (RL) × 8 (FH) mm^3) was positioned on the anterior body of the corpus callosum as shown in **Figure 1**. The diffusion-weighting gradients were applied in two directions: a right-left direction in the VOI frame, mostly parallel to the direction of the callosal fibers (direction [1,0,0]), and a direction mostly perpendicular to the callosal fibers (direction [0,-1,1]), as shown in **Figure 1A and B**. The center frequency was set to the tNAA singlet peak at 2.0 ppm. Water suppression was performed using two frequency-selective excitation pulses, each followed by a dephasing gradient before metabolite excitation. Pencil beam second-order shimming was performed, resulting in a typical tNAA line width of 10 Hz. A peripheral pulse unit was used in order to gate data acquisition to the cardiac cycle, thereby minimizing signal fluctuations due to cardiac pulsation. The parameters for DW-MRS acquisitions were: TE = 121 ms, TR = 3 cardiac cycles (about 3000 ms), cardiac trigger delay = 300 ms, number of time-domain points = 1024, spectral width = 3000 Hz, gradient duration (δ) = 37 ms, bipolar gap = 16 ms, diffusion time (Δ) = 60.5 ms with 5 different gradient amplitudes resulting in b-values of 212, 651, 1335, 2262, and 3462 s/mm^2 in the [1,0,0] direction and 440,1336, 2718, 4586, and 6945 s/mm^2 in the [0,-1,1] direction. The total number of spectra per diffusion condition was 32, resulting in a total scan time of 10~15 minutes. Following this scan, a shorter scan (fewer signal averages) with identical VOI position and diffusion conditions was performed without water suppression and with the center frequency set at the water resonance frequency. These spectra were used for eddy-current correction in the post-processing stage.

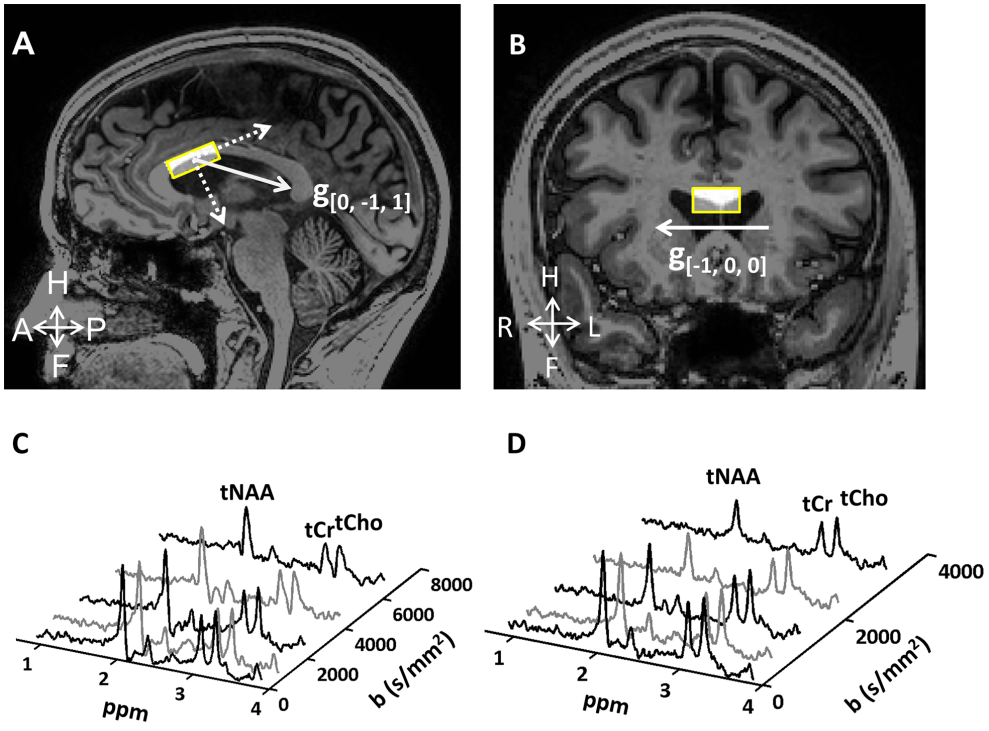

Figure 1. The position of the volume of interest in sagittal (A) and coronal (B) views. Gradients applied in directions approximately perpendicular (A) and parallel (B) to the callosal fibers are shown in solid lines. Typical spectra acquired with diffusion weighting in the [0, -1, 1] and the [1, 0, 0] directions are shown as a function of b-value in panels (C) and (D), respectively. Line broadening of 5 Hz was applied for display purposes.

DW-MRS Processing

All spectral pre-processing was performed with custom codes in MATLAB® release R2014b (Mathworks, Natick, MA, USA). Spectral preprocessing consisted of correcting DW-MRS data for eddy currents, zero-order phasing, correction of frequency drift for individual acquisitions, and removal of the residual water peak: averaged spectra were generated for each condition.(29) **Figure 1C and D** show typical sets of diffusion-weighted spectra obtained with diffusion-weighting in the (1, 0, 0) direction (**Figure 1C**) and the (0,-1, 1) direction (**Figure 1D**), respectively and from a healthy control subject. The resulting spectra were quantified with LCModel.(30) Cramér–Rao lower bound (CRLB) values were used to evaluate the quality of the spectra for each diffusion condition, and the acceptance threshold for DW-MRS data inclusion was set at CRLB < 20%. Based on this, data sets from one NP-SLE subject and one SLE subject were excluded from the tNAA analysis.

The LCModel spectral estimates were used to calculate the diffusivity (D_{par}) along the [1,0,0] direction (roughly parallel to the callosal fibers) and diffusivity (D_{perp}) along the [0,-1,1] direction (roughly perpendicular to the callosal fibers) for tNAA, tCr and tCho. These were calculated by performing a linear fit of the natural logarithm of the DW-MRS signal amplitudes as a function of the diffusion weighting value **b**, assuming a monoexpoential decay of the signal as a function of b in each direction:

$$ln\left(\frac{S_{b,i}}{S_{b_0}}\right) = -b_i \cdot D_i$$

where is the measured signal in direction **i**, is the signal without diffusion weighting, b_i is the value of b in the direction **i**, and D_i is the calculated diffusion coefficient for direction **i**. Even though it is possible that the metabolite diffusion-weighted signal decay displays non-monoexponential behavior at very high values of b, our previous work has shown that in the range of b values used in this study the assumption of monoexponentiality is valid and diffusivity values are reproducible.(13,29) An average of D_{par} and D_{perp} was calculated to assess the average diffusivity (D_{avg}) for tNAA, tCr and tCho. The quality of the linear fittings was evaluated via calculation of the coefficient of determination and an acceptance threshold was set at 75%, leading to exclusion of D_{avg}(tCr) values obtained from two patients with NP-SLE and one patient with SLE.

Image Processing

DTI volumes were motion-corrected with ExploreDTI and further processed with the DTI toolbox (31) of the FMRIB Software Library (FSL release 5.0, http://www.fmrib.ox.ac.uk/fsl/) to obtain the following DTI measures for each subject: fractional anisotropy (FA), mean diffusivity (MD), axial diffusivity (AD) and radial diffusivity (RD). These DTI metrics were further analyzed with tract based spatial statistics (TBSS).(32) Statistical differences between NP-SLE patients, SLE patients and HC were assessed in FA-MNI152 standard space using 5000 permutations and were corrected for multiple comparison based on threshold-free cluster enhancement(Winkler **et al.** 2014). One SLE patient data set was excluded due to poor registration to FA-MNI152.

T_1-weighted images were used for tissue segmentation within the VOI.(29) Fractional anisotropy maps were registered to the T_1-weighted image of the same subject first by affine transformation using FSL FLIRT and subsequently by non-rigid transformation using FNIRT. (33-35) The inverse transformation matrices generated were used to register the DW-MRS VOI to the DTI space. Subsequently, the registration procedure in TBSS was applied to transform each VOI to MNI152 space.

T_1-weighted volumes were further processed in FreeSurfer (http://surfer.nmr.mgh.harvard.edu/) and the intracranial volume, total brain volume, center corpus callosum volume and mid-anterior corpus callosum volume were calculated for each subject. To evaluate whole brain and callosal atrophy due to SLE and NP-SLE, total brain volume, center corpus callosum volume and mid-anterior corpus callosum volume were normalized according to the intracranial volume of the same subject.

Statistical Analyses

Patients with NP-SLE and those with SLE were compared with respect to demographic characteristics, presence of autoantibodies and ACR criteria and current medication using chi-square tests and ANOVA or Mann-Whitney tests when appropriate. Primary dependent measures included in the statistics were D_{avg}(tNAA), D_{avg}(tCr), D_{avg}(tCho). Shapiro-Wilk test was used to examine the distribution of variables, and resulted in all being normally distributed. Equality of variances of the different groups was assessed using Levene's test. Between-group differences on all D_{avg} values were evaluated using one-wayANOVAs (pairwise comparisons). $P < 0.05$ was considered to represent statistically significant differences. Bonferroni's correction was used to correct for multiple comparisons. Analysis of covariance was performed to analyse the influence of age and SLEDAI-2K on the differences of mean D_{avg} values between groups. As SLEDAI-2K and SDI scores were not normally distributed, correlations between the metabolite D_{avg} measurements and SLEDAI-2K score and SDI score were evaluated with Spearman's rank correlation. Correlations between SLE duration and D_{avg} values were assessed with Pearson's correlation test. All statistical analyses were performed with SPSS version 20.0 for Windows (IBM SPSS statistics, Chicago, IL, USA). Scattered plots were generated using GraphPad Prism 5 for windows, version 5.01, GraphPad Software, USA.

RESULTS

DW-MRS results

Average metabolite D_{avg} values for the NP-SLE, SLE and healthy control groups are shown in **Table 2** and group D_{avg} data for the three population groups are displayed in **Figure 2**. When all three groups were compared with ANOVA with age included as a covariate, significant differences were found in D_{avg}(tCho) ($P = 0.006$) and D_{avg}(tCr) ($P = 0.030$). No significant differences were found in D_{avg}(tNAA) among the groups.

Table 2: Metabolite D_{avg} values for NPSLE patients, SLE patients and healthy controls.

	NPSLE patients (n = 13)	SLE patients (n = 16)	Healthy controls (n=19)	% increase in NPSLE vs HC
D_{avg}(tNAA) μm²/s	0.24 ± 0.02	0.23 ± 0.02	0.23 ± 0.02	7%
D_{avg}(tCr) μm²/s	0.20 ± 0.03**	0.18 ± 0.03	0.17 ± 0.02	18%
D_{avg}(tCho) μm²/s	0.14 ± 0.03*	0.13 ± 0.02	0.12 ± 0.02	14%

*p-value<0.05 versus healthy controls **p-value<0.01 versus healthy controls

Pairwise comparisons showed that in patients with NP-SLE, D_{avg}(tCr) and D_{avg}(tCho) were significantly higher than in healthy controls after correction for age (mean D_{avg}(tCr) in NP-SLE = 0.202 ± 0.032μm²/ms, mean D_{avg}(tCr) in healthy controls = 0.171 ± 0.024μm²/ms, *P* = 0.018 and mean D_{avg}(tCho) in NP-SLE = 0.142 ± 0.031μm²/ms, mean D_{avg}(tCho) in healthy controls = 0.124 ± 0.018μm²/ms, *P* = 0.044). No significant difference was found in D_{avg}(tNAA) values between patients with NP-SLE and healthy control subjects. No significant differences were observed in any metabolite Davg between NP-SLE and SLE or between SLE and healthy control groups. SLEDAI-2K was used as a covariate when patients with SLE and those with NP-SLE were compared. When all SLE patients, with and without past CNS involvement, were grouped together and compared to healthy control subjects, D_{avg}(tCr) and D_{avg}(tCho) remained significantly higher in patients with SLE than in healthy control subjects after correcting for age [mean D_{avg}(tCr) in all SLE patients = 0.190 ± 0.034μm²/ms, mean D_{avg}(tCr) in healthy controls = 0.171 ± 0.024μm²/ms, *P* = 0.060 and mean D_{avg}(tCho) in all SLE patients = 0.135 ± 0.028μm²/ms, mean D_{avg}(tCho) in healthy controls = 0.124 ± 0.018μm²/ms, *P* = 0.008].

Average diffusion coefficients of all metabolites showed a link to disease activity in both the patients with SLE and those with NP-SLE. When all patients with SLE were pooled together, regardless of their neuropsychiatric status, SLEDAI-2K scores correlated positively with D_{avg}(tNAA) (r = 0.412, *P* = 0.033), D_{avg}(tCr) (r = 0.405, *P* = 0.040) and D_{avg}(tCho) (r = 0.480, *P* = 0.008). Scatter plots of the SLEDAI-2K scores of all patients as a function of metabolite D_{avg} values are shown in **Figure 3**. When patients with SLE and those with NP-SLE categorized as SLE-active (SLEDAI-2 ≥ 8, n = 5) were compared to healthy control subjects, statistically significant differences in D_{avg}(tCr) were found [D_{avg}(tCr) in SLE-active = 0.216 ± 0.038μm²/ ms, D_{avg}(tCr) in healthy controls = 0.171 ± 0.024μm²/ms, *P* = 0.006], as well as in D_{avg}(tCho) [D_{avg}(tCho) in SLE active = 0.154 ± 0.037μm²/ms, D_{avg}(tCho) in healthy controls = 0.124 ± 0.018μm²/ms, *P* = 0.006] after correcting for age. No correlation was found between metabolite D_{avg} values and SLE duration or SDI scores.

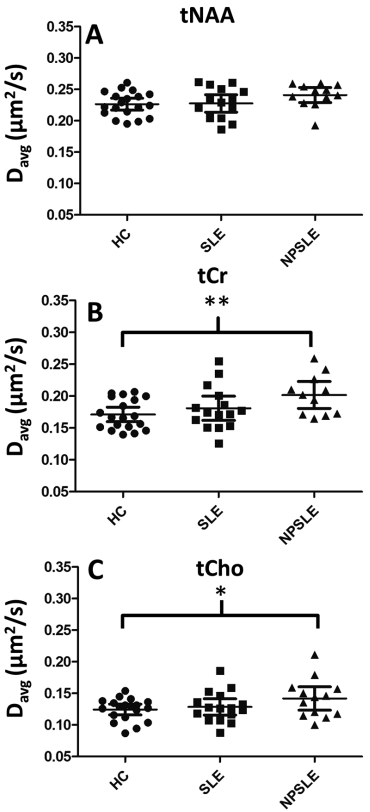

Figure 2. Metabolite Davg values for healthy controls subjects and patients with SLE and patients with NPSLE. Davg (tNAA), Davg (tCr) and Davg (tCho) data are shown in A, B and C, respectively. Statistically significant differences are shown as *P<0.05 and **P<0.01. No significant differences were found between SLE and healthy control subjects, or between NPSLE and SLE in any of the metabolite Davg values. HC = healthy controls.

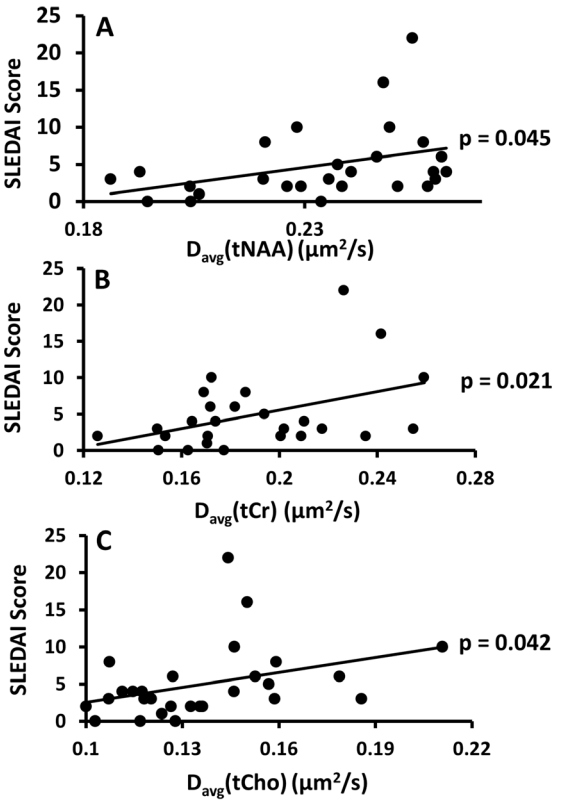

Figure 3. Correlation of metabolite Davg values with patient SLEDAI-2K scores. The resulting Spearman's rank correlation r and significance of the correlations are shown for Davg (tNAA) (A), Davg(tCr) (B) and Davg(tCho)

DTI and volumetric results

Significantly lower FA, higher MD and higher RD were found throughout white matter in the NP-SLE patient group compared to the healthy control and SLE groups, including the callosal region within the DW-MRS volume of interest ($P < 0.05$). **Figure 4** shows maps of statistically significant differences ($P < 0.05$) in DTI measures overlaid on the MNI152 T1weighted image, and the cumulative DW-MRS volume of interest (i.e. the sum of all the individual volumes of interest following transformation from the individual subject coordinates to the FA-MNI152 coordinates). The voxels with significantly higher mean and radial diffusivity values in the patients with NP-SLE compared to healthy controls are shown in blue and voxels with lower fractional anisotropy values in patients with NP-SLE compared to healthy controls are shown in red. No significant differences were found in any DTI measure between SLE patients (with and without past CNS involvement) and healthy control subjects. No significant differences were found in corpus callosum volumes or total brain volumes between patients with SLE or those with NP-SLE, and healthy control subjects.

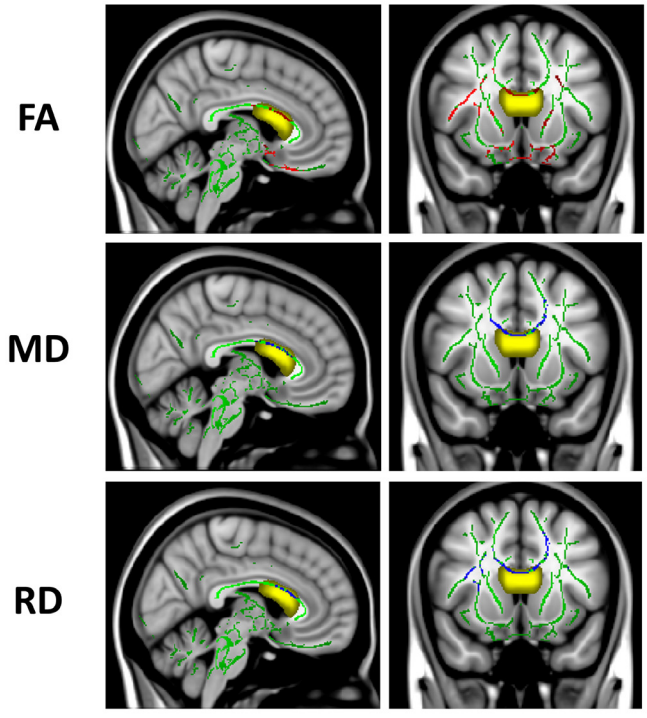

Figure 4. Tract-based spatial statistics results showing regions with statistically significant differences in DTI measures in the white matter skeleton of patients with NPSLE and healthy control subjects (P<0.05). Maps are shown for one sagittal (left) and one coronal (right) slice in MNI152 space. The mean fractional anisotropy skeleton is shown in green, regions with higher values in the patients with NPSLE compared to healthy control subjects are shown in blue and regions with lower values in patients with NPSLE compared to healthy control are shown in red. Cumulative volume of interests chosen for DW-MRS of patients with NPSLE and healthy controls are shown in yellow.
FA = fractional anisotropy; MD = mean diffusivity; RD = radial diffusivity.

DISCUSSION

This is the first study to address cell-specific microstructural alterations in the brain of SLE patients with DW-MRS at ultrahigh field. This study focused on measuring the diffusion properties of two predominantly glial metabolites, tCr and tCho, and one exclusively axonal/neuronal metabolite, tNAA. The most salient finding in this study is the strong and consistent link between both D_{avg}(tCr) and D_{avg}(tCho) and disease state, with respect to disease activity and to past CNS involvement, suggesting glial involvement in the brain of these patients. Two potential pathological mechanisms that can explain the significantly higher tCr and tCho diffusivities found in NP-SLE patients are inflammation-mediated morphological changes in microglia and astrocytes, and intracellular edema, which would affect both glia and neurons/axons.(36-38)

Astrocytic and microglial reactivity in response to inflammation and/or ischemia are both highly consistent with an increase in intracellular diffusivity in glia. Reactivity-related cellular hypertrophy and thickening of the processes near the soma (especially in astrocytes) (39) would result in an increase of the intracellular space, and a decrease in molecular crowding and intracellular tortuosity, leading to increased diffusivity in the cytosol. The pathogenesis of NP-SLE is thought to involve various immune and inflammatory processes that can lead to neuronal injury and vasculopathy.(40) The inflammatory response to injury likely results in glial reactivity and cellular hypertrophy, especially in microglia and astrocytes.(37,38) Histolopathological investigations of brains of NP-SLE patients, confirm the widespread presence of reactive microglia and astrocytes, as well as of lipid-laden macrophages among the heterogeneous pathological phenomena.(36) Furthermore, the correlation of in vivo MRS results with histological results from the same patients suggest: (a) an association between an increase in tCho concentrations and gliosis, vasculopathy and edema; (b) possible association of tCr with gliosis and reduced neuronal/axonal density; and (c) an association between lower tNAA concentrations and a decrease in neuronal/axonal density.(36)

The higher D_{avg}(tNAA) values found in NP-SLE patients compared to HC may be attributed to changes in cytosolic viscosity in axons due either to neuronal/axonal damage or to cytotoxic edema, both of which are seen in the histopathology of brains of NP-SLE patients.(8) Higher D_{avg}(tNAA) has also been observed in a study of patients with schizophrenia where it was hypothesized that inflammatory processes may play a role.(41) On the other hand, lower tNAA parallel diffusivity values were found in multiple sclerosis (MS) patients compared to HC in a study focused on myelin and axonal changes in the corpus callosum.(19) It is likely that the different behaviors in tNAA diffusivity seen in MS and in NP-SLE reflect different intra-axonal pathological mechanisms associated with these two diseases. Central to MS are demyelination and axonopathy.(42,43) As demyelination has no direct effect on diffusion in

the intra-axonal space, it has been hypothesized that in MS the decrease in tNAA axosolic diffusivity stemmed from axonal damage that included unusual patterns of neurofilament phosphorylation and packing compared to normal tissue, and a less organized axoskeleton and/or problems with axonal transport.(44) In contrast to findings in MS, histology of patients with NP-SLE have shown that cerebral edema occurs much more frequently than axonal/neuronal loss (8) and is thus more compatible with the increase in axosolic diffusivity, as evidenced by the increase in D_{avg}(tNAA) observed in our study.

The high correlation in all SLE/NP-SLE patients between SLE disease activity, as quantified by the SLEDAI-2K score, and D_{avg}(tCr) and D_{avg}(tCho) suggests that the SLE-related peripheral inflammation and autoimmune response may have effect on the brain, independent of overt clinical CNS involvement in SLE. Additionally, significant correlation of D_{avg}(tNAA) values with SLEDAI-2K scores suggests a permanent or continuous damage to axons correlated with high SLE activity. This is further corroborated by the finding that patients with higher disease activity (those we defined as SLE-active) have higher metabolite diffusivity levels and higher statistical significance in the difference in metabolite diffusivity compared to HC. A previous MRS study in NP-SLE/SLE has shown a significantly lower tNAA/tCr level in SLE patients with a high SLEDAI-2K score, and that the level of tNAA/tCr was renormalized in follow-up for patients who were no longer SLE-active, regardless of their NP status.(11) This finding suggests a pathological mechanism, attributed by the authors to neuronal dysfunction that affects both neurons and axons, the degree of which depends on SLE disease activity, but which is essentially reversible in nature. In our view, and based on our corroborative findings, we attribute this finding to intracellular/intraaxonal edema. It has been suggested that inflammation outside the brain can prime microglia and result in microglial activation for several weeks.(45) Our findings, as well as those described by Appenzeller et al.(46) support the view that systemic inflammation affects the brain in NP-SLE, and the underlying mechanism by which this occurs, e.g. potential disruption of the blood brain barrier in SLE (47), should be further investigated.

Metabolite apparent diffusion coefficient (ADC) values found in healthy controls in this study are similar to those reported in previous DW-MRS studies performed on a similar region of the corpus callosum at 7 tesla and 3 tesla.(21,29) A recently published robustness and reproducibility study of DW-MRS in the anterior body of the corpus callosum, aimed to provide guidelines for DW-MRS acquisition for clinical studies such as the one presented here. Using power calculations based on actual data it was estimated that in order to observe a 10% difference in D_{avg} values for tNAA, tCr and tCho in a case-control study, nine, four and twelve subjects, respectively, are sufficient.(29) In this current study we observed a 7% increase in D_{avg}(tNAA), 19% increase in D_{avg}(tCr) and 14% in D_{avg}(tCho) in NP-SLE patients compared to HC, with thirteen and nineteen subjects per group, respectively. This

suggests that it is feasible to observe reliably the disease effect on metabolite D_{avg} reported here. Moreover, based on our power estimation, the number of subjects required to observe reliably a difference in D_{avg}(tCho) is higher than that required for D_{avg}(tNAA). This further supports the notion that our findings indicate a larger effect size for glial than for axonal involvement in SLE/NP-SLE. The DTI results are also consistent with previous studies on SLE and NP-SLE.(4,5,7) Significantly lower fractional anisotropy values in the anterior body of the corpus callosum of patients with NP-SLE compared to healthy controls were previously reported in a DTI study on NP-SLE where region of interest analysis was performed.(48) This study also included MRS measurements in normal appearing parietal white matter, and no differences in glial metabolite concentrations (tCr, tCho) between patients with NP-SLE and healthy controls were reported. Although changes in concentrations of glial metabolites have been linked to glial reactivity and neuroinflammation (49) this may suggest that the diffusion properties of glial metabolites are more sensitive to glial reactivity than their cellular concentration. Atrophy measurements did not show any significant callosal or global atrophy in the patient population, possibly stemming from a type II error due to the small size of the cohort.

There were several challenges and limitations to the study. The main (unmet) challenge of this study was to scan patients with active NP symptoms at the time of the scan, as well as to include more patients with high SLE disease activity. Low incidence of active NP-SLE was a factor, as well as significant potential discomfort to patients with clinically overt NP symptoms, preventing these patients from being involved in a research study that is not part of the routine clinical procedure. Another limitation of this study is the small number of patients per specific neuropsychiatric syndrome. This is a generally recognized problem in NP-SLE studies, mainly related to the low prevalence and the high heterogeneity of NP-SLE. Subsequently, definite conclusions concerning the relationship between DW-MRS findings and NP-SLE syndromes cannot be drawn. In our patient cohort, the relative low number of patients with antiphospholipid syndrome made it difficult to evaluate the effect of ischaemic/vascular changes on metabolite diffusion. As a consequence, we did not separately analyze changes in ischaemic and inflammatory patients with NP-SLE. Future studies will focus on separate evaluation of the effects of neuropsychiatric activity, ischaemic and inflammatory effects. The study would have benefitted from a separate MRS acquisition at short echo time, for an accurate evaluation of the metabolite concentrations in the same volume of interest, together with additional cell-specific metabolites such as glutamate, glutamine and myo-inositol.

In conclusion, the results presented in this study show for the first time that intracellular metabolite diffusion reflective of glial and neuronal/axonal involvement can be measured by DW-MRS in a complex autoimmune disease such as SLE/NP-SLE. This technique has great

potential for the study of the aetiology of disease-related changes in tissue microstructure of patients with SLE/NP-SLE. We believe that if incorporated in a comprehensive diagnostic scanning protocol together with existing microstructural MRI tools, such as DTI, MTI and susceptibility weighted imaging, DW-MRS can contribute to the diagnostic process of these patients and may help unravel underlying pathogenic mechanisms in this complex disease.

REFERENCES

1. Jeltsch-David H, Muller S. Neuropsychiatric systemic lupus erythematosus: pathogenesis and biomarkers. Nat Rev Neurol 2014; 10: 579–96.
2. Luyendijk J, Steens SC, Ouwendijk WJ, Steup-Beekman GM, Bollen EL, van der Grond J, et al. Neuropsychiatric systemic lupus erythematosus: lessons learned from magnetic resonance imaging. Arthritis Rheum 2011; 63: 722–32.
3. Bosma GP, Rood MJ, Zwinderman AH, Huizinga TW, van Buchem MA. Evidence of central nervous system damage in patients with neuropsychiatric systemic lupus erythematosus, demonstrated by magnetization transfer imaging. Arthritis Rheum 2000; 43: 48–54.
4. Emmer BJ, Veer IM, Steup-Beekman GM, Huizinga TW, van der Grond J, van Buchem MA. Tract-based spatial statistics on diffusion tensor imaging in systemic lupus erythematosus reveals localized involvement of white matter tracts. Arthritis Rheum 2010; 62: 3716–21.
5. Jung RE, Caprihan A, Chavez RS, Flores RA, Sharrar J, Qualls CR, et al. Diffusion tensor imaging in neuropsychiatric systemic lupus erythematosus. BMC Neurol 2010; 10: 65.
6. Jung RE, Chavez RS, Flores RA, Qualls C, Sibbitt WL Jr, Roldan CA. White matter correlates of neuropsychological dysfunction in systemic lupus erythematosus. PLoS One 2012; 7: e28373.
7. Ercan E, Ingo C, Tritanon O, Magro-Checa C, Smith A, Smith S, et al. A multimodal MRI approach to identify and characterize microstructural brain changes in neuropsychiatric systemic lupus erythematosus. Neuroimage Clin 2015; 8: 337–44.
8. Sibbitt WL, Brooks WM, Kornfeld M, Hart BL, Bankhurst AD, Roldan Ca. Magnetic resonance imaging and brain histopathology in neuropsychiatric systemic lupus erythematosus. Semin Arthritis Rheum 2010; 40: 32–52.
9. Sibbitt WL Jr, Haseler LJ, Griffey RR, Friedman SD, Brooks WM. Neurometabolism of active neuropsychiatric lupus determined with proton MR spectroscopy. Am J Neuroradiol 1997; 18: 1271–7.
10. Axford JS. Sensitivity of quantitative 1H magnetic resonance spectroscopy of the brain in detecting early neuronal damage in systemic lupus erythematosus. Ann Rheum Dis 2001; 60: 106–11.
11. Appenzeller S, Li LM, Costallat LT, Cendes F. Evidence of reversible axonal dysfunction in systemic lupus erythematosus: a proton MRS study. Brain 2005; 128: 2933–40.
12. Nicolay K, Braun KP, Graaf RA, Dijkhuizen RM, Kruiskamp MJ. Diffusion NMR spectroscopy. NMR Biomed 2001; 14: 94–111. Perry VH, Holmes C. Microglial priming in neurodegenerative disease. Nat Rev Neurol 2014; 10: 217–24.
13. Kan HE, Techawiboonwong A, van Osch MJ, Versluis MJ, Deelchand DK, Henry PG, et al. Differences in apparent diffusion coefficients of brain metabolites between grey and white matter in the human brain measured at 7 T. Magn Reson Med 2012; 67: 1203–9.
14. Urenjak J, Williams SR, Gadian DG, Noble M. Proton nuclear magnetic resonance spectroscopy unambiguously identifies different neural cell types. J Neurosci 1993; 13: 981–9.
15. Choi JK, Dedeoglu A, Jenkins BG. Application of MRS to mouse models of neurodegenerative illness. NMR Biomed 2007; 20: 216–37.
16. Harada M, Uno M, Hong F, Hisaoka S, Nishitani H, Matsuda T. Diffusion-weighted in vivo localized proton MR spectroscopy of human cerebral ischemia and tumor. NMR Biomed 2002; 15: 69–74.
17. Zheng DD, Liu ZH, Fang J, Wang XY, Zhang J. The effect of age and cerebral ischemia on diffusion-weighted proton MR spectroscopy of the human brain. Am J Neuroradiol 2012; 33: 563–8.
18. Colvin DC, Yankeelov TE, Does MD, Yue Z, Quarles C, Gore JC. New insights into tumor microstructure using temporal diffusion spectroscopy. Cancer Res 2008; 68: 5941–7.
19. Wood ET, Ronen I, Techawiboonwong A, Jones CK, Barker PB, Calabresi P, et al. Investigating axonal damage in multiple sclerosis by diffusion tensor spectroscopy. J Neurosci 2012; 32: 6665–9.
20. Ronen I, Budde M, Ercan E, Annese J, Techawiboonwong A, Webb A. Microstructural organization of axons in the human corpus callosum quantified by diffusion-weighted magnetic resonance spectroscopy of N-acetylaspartate and post-mortem histology. Brain Struct Funct 2014; 219: 1773–85.
21. Ronen I, Ercan E, Webb A. Axonal and glial microstructural information obtained with diffusion-weighted magnetic resonance spectroscopy at 7T. Front Integr Neurosci 2013; 7: 13.
22. Tan EM, Cohen AS, Fries JF, Masi AT, McShane DJ, Rothfield NF, et al. The 1982 revised criteria for the classification of systemic lupus erythematosus. Arthritis Rheum 1982; 25: 1271–7.
23. Hochberg MC. Updating the American College of Rheumatology revised criteria for the classification of systemic lupus erythematosus. Arthritis Rheum 1997; 40: 1725.
24. Zirkzee EJ, Steup-Beekman GM, van der Mast RC, Bollen EL, van der Wee NJ, Baptist E, et al. Prospective study of clinical phenotypes in neuropsychiatric systemic lupus erythematosus; multidisciplinary approach to diagnosis and therapy. J Rheumatol 2012; 39: 2118–26.

25. The American College of Rheumatology nomenclature and case definitions for neuropsychiatric lupus syndromes. Arthritis Rheum 1999; 42: 599–608.
26. Gladman DD, Ibanez D, Urowitz MB. Systemic lupus erythematosus disease activity index 2000. J Rheumatol 2002; 29: 288–91.
27. Gladman DD, Goldsmith CH, Urowitz MB, Bacon P, Fortin P, Ginzler E, et al. The Systemic Lupus International Collaborating Clinics/ American College of Rheumatology (SLICC/ACR) Damage Index for Systemic Lupus Erythematosus International Comparison. J Rheumatol 2000; 27: 373–6.
28. Gladman DD, Urowitz MB, Goldsmith CH, Fortin P, Ginzler E, Gordon C, et al. The reliability of the Systemic Lupus International Collaborating Clinics/ American College of Rheumatology Damage Index in patients with systemic lupus erythematosus. Arthritis Rheum 1997; 40: 809–13.
29. Wood ET, Ercan AE, Branzoli F, Webb A, Sati P, Reich DS, et al. Reproducibility and optimization of in vivo human diffusionweighted MRS of the corpus callosum at 3T and 7T. NMR Biomed 2015; 28: 976–87.
30. Provencher SW. Estimation of metabolite concentrations from localized in vivo proton NMR spectra. Magn Reson Med 1993; 30: 672–9.
31. Behrens TE, Woolrich MW, Jenkinson M, Johansen-Berg H, Nunes RG, Clare S, et al. Characterization and propagation of uncertainty in diffusion-weighted MR imaging. Magn Reson Med 2003; 50: 1077–88.
32. Smith SM, Jenkinson M, Johansen-Berg H, Rueckert D, Nichols TE, Mackay CE, et al. Tract-based spatial statistics: voxelwise analysis of multi-subject diffusion data. Neuroimage 2006; 31: 1487–505.
33. Jenkinson M, Bannister P, Brady M, Smith S. Improved optimization for the robust and accurate linear registration and motion correction of brain images. Neuroimage 2002; 17: 825–41.
34. Jenkinson M, Smith S. A global optimisation method for robust affine registration of brain images. Med Image Anal 2001; 5: 143–56.
35. Andersson JLR, Jenkinson M, Smith S. (2010). Non-linear registration, aka spatial normalisation. FMRIB technical report TR07JA2, from www.fmrib.ox.ac.uk/analysis/techrep.
36. Brooks WM, Sibbitt WL Jr, Kornfeld M, Jung RE, Bankhurst AD, Roldan CA. The histopathologic associates of neurometabolite abnormalities in fatal neuropsychiatric systemic lupus erythematosus. Arthritis Rheum 2010; 62: 2055–63.
37. Graeber MB, Streit WJ. Microglia: biology and pathology. Acta Neuropathol 2010; 119: 89–105.
38. Sofroniew MV, Vinters HV. Astrocytes: biology and pathology. Acta Neuropathol 2010; 119: 7–35. 39. Sofroniew MV. Molecular dissection of reactive astrogliosis and glial scar formation. Trends Neurosci 2009; 32: 638–47.
39. Sofroniew MV. Molecular dissection of reactive astrogliosis and glial scar formation. Trends Neurosci 2009; 32:638-47.
40. Popescu A, Kao AH. Neuropsychiatric systemic lupus erythematosus. Curr Neuropharmacol 2011; 9: 449–57.
41. Du F, Cooper AJ, Thida T, Shinn AK, Cohen BM, Ongur D. Myelin and axon abnormalities in schizophrenia measured with magnetic resonance imaging techniques. Biol Psychiatry 2013; 74: 451–7.
42. Petzold A, Tozer DJ, Schmierer K. Axonal damage in the making: neurofilament phosphorylation, proton mobility and magnetisation transfer in multiple sclerosis normal appearing white matter. Exp Neurol 2011; 232: 234–9.
43. Stadelmann C, Wegner C, Bruck W. Inflammation, demyelination, and degeneration - recent insights 44. Petzold A, Gveric D, Groves M, Schmierer K, Grant D, Chapman M, et al. Phosphorylation and compactness of neurofilaments in multiple sclerosis: indicators of axonal pathology. Exp Neurol 2008; 213: 326–35.
44. Petzold A, Gveric D, Groves M, Schmierer K, Grant D, Chapman M, et al. Phosphorylation and compactness of neurofilaments in multiple sclerosis: indicators of axonal pathology. Exp Neurol 2008; 213:326-35.
45. Perry VH, Holmes C. Microglial priming in neurodegenerative disease. Nat Rev Neurol 2014;10:217-24.
46. Appenzeller S, Costallat LT, Li LM, Cendes F. Magnetic resonance spectroscopy in the evaluation of central nervous system manifestations of systemic lupus erythematosus. Arthritis Rheum 2006; 55: 807–11.
47. Abbott NJ, Mendonca LL, Dolman DE. The blood-brain barrier in systemic lupus erythematosus. Lupus 2003; 12: 908–15. ACR.
48. Zimny AM, Szmyrka-Kaczmarek P, Szewczyk J, Bladowska A, Pokryszko-Dragan E, Gruszka P, et al. In vivo evaluation of brain damage in the course of systemic lupus erythematosus using magnetic resonance spectroscopy, perfusion-weighted and diffusion tensor imaging. Lupus 2014; 23: 10–19.
49. Chang L, Munsaka SM, Kraft-Terry S, Ernst T. Magnetic resonance spectroscopy to assess neuroinflammation and neuropathic pain. J Neuroimmune Pharmacol 2013; 8: 576–93.

7